

Low resistivity *p*-ZnO films fabricated by sol-gel spin coating

Yongge Cao,^{a)} Lei Miao, Sakae Tanemura, Masaki Tanemura, Yohei Kuno, and Yasuhiko Hayashi

Department of Environmental Technology and Urban Planning, Nagoya Institute of Technology, Showa-ku, Nagoya 466-8555, Japan

(Received 28 December 2005; accepted 22 May 2006; published online 22 June 2006)

N-doped and In-N-codoped ZnO films were fabricated on quartz glass substrate by sol-gel spin coating. Their *p*-type conductivities were characterized by the Hall measurements, revealing low resistivities of the order of $10^{-1} \Omega \text{ cm}$. Thin-film junctions comprising an undoped ZnO layer and a N-doped ZnO layer displayed the typical rectifying characteristics, suggesting formation of *p-n* homojunctions at the interfaces. © 2006 American Institute of Physics. [DOI: 10.1063/1.2215618]

ZnO has been extensively investigated due to its potentials in optoelectronic applications. It has a wide band gap (3.37 eV) and a large exciton binding energy (60 meV).^{1,2} To realize ZnO-based optoelectronic devices, it is essential to fabricate high quality *p*-ZnO films. Although many reports claimed realizations of *p*-type ZnO films and *p-n* homojunctions,^{3–13} highly reproducible *p*-ZnO film with excellent electronic properties is still absent.¹⁴ Efficient optical emission from ZnO *p-n* diode is extremely difficult to realize¹⁴ due to the problems associated with low solubility of acceptor dopants, self-compensation effects, and formation of undesirable deep levels.^{14,15} The reported data for *p*-ZnO films all showed a high resistivity in the range of 10^0 – $10^4 \Omega \text{ cm}$ (Refs. 3–7 and 9–11) except for the one where a remarkably low resistivity of $1.7 \times 10^{-2} \Omega \text{ cm}$ and a high mobility of $155 \text{ cm}^2 \text{ V}^{-1} \text{ s}^{-1}$ were measured by Bian *et al.* for a N-In-codoped ZnO film grown on *n*-type Si(100) substrate.¹² This latter result is, however, controversial in the sense that the effect of conductive substrate on Hall data is unclear.^{13,14,16}

To verify the low resistivity *p*-ZnO films and the effect of codoping, we prepared both N-doped and In-N-codoped ZnO films using a simple method of sol-gel spin coating.¹⁷ ZnO *p-n* homojunctions were also made and characterized by Hall and *I-V* measurements. In order to eliminate the influence of conductive substrates and to conveniently carry out optical measurements, transparent insulating fused quartz glass was used as a substrate for all the films. We achieved both *p*-type ZnO films and *p-n* homojunction by sol-gel spin coating, which has never been reported until now.¹⁴

To prepare undoped, N-doped, and In-N-codoped ZnO films, zinc acetate 2-hydrate [$\text{Zn}(\text{CH}_3\text{COO})_2 \cdot 2\text{H}_2\text{O}$] was firstly dissolved into 2-methoxyethanol solution with the addition of sol stabilizers monoethanolamine (MEA). Ammonia acetate and standard indium nitrite solution were used as the nitrogen and indium sources, respectively. The three kinds of clear solutions, with a concentration of 0.5M zinc acetate and 1:1 molar ratio of MEA/zinc acetate, were prepared through reflux at 80 °C for 3 h. The atomic ratio of Zn/N is 1:3 (for ZnO:N film) and that of Zn/N/In is 1:3:0.1 (for ZnO:N:In film). The respective sols were spin coated on glass substrates at 3000 rpm. The precursor films were preheated at 280 °C for 10 min in air in order to remove the

volatile materials. The process of coating and preheating was repeated for several times before the required film thickness ($\sim 400 \text{ nm}$) was met. Preannealing for 1.5 h at 550 and 450 °C in air was implemented for both undoped and doped ZnO films, respectively. To realize good crystallinity, a post-annealing procedure at 550 °C in pure O₂ atmosphere for another 1.5 h was also adopted.

The crystalline phase and orientation of the ZnO films were determined by x-ray diffraction (XRD) (using the Cu *K* α radiation in RINT 2000, Rigaku Co.). Figure 1 shows the XRD results of the undoped, N-doped, and In-N-codoped ZnO films. It can be observed that the three ZnO films all exhibit the wurtzite structural phase with the preferential orientation of (0002). The absence of the other peaks in the XRD spectra suggests that there is no inclusion of additional phases such as InN, In₂O₃, Zn₃N₂, Zn_xO_yN_z, and ZnIn₂O₄ compounds, some of which were observed in Ga-doped ZnO films.¹⁸ A clear low-angle shift of the (0002) peak is identified (see inset of Fig. 1), which implies that d_{0002} increases upon the substitution of O($r_{\text{O}}=0.65 \text{ \AA}$) by N($r_{\text{N}}=0.75 \text{ \AA}$) or Zn($r_{\text{Zn}}=1.53 \text{ \AA}$) by In($r_{\text{In}}=2.00 \text{ \AA}$). An apparent decrease in crystallinity was also observed as suggested by the decrease in intensity of the (0002) peak with increasing N-doping.

Room temperature (RT) transmittance spectroscopy (UV-vis spectrophotometer; JASCO-V750, spectral range of 300–600 nm) has been conducted measuring the band gaps

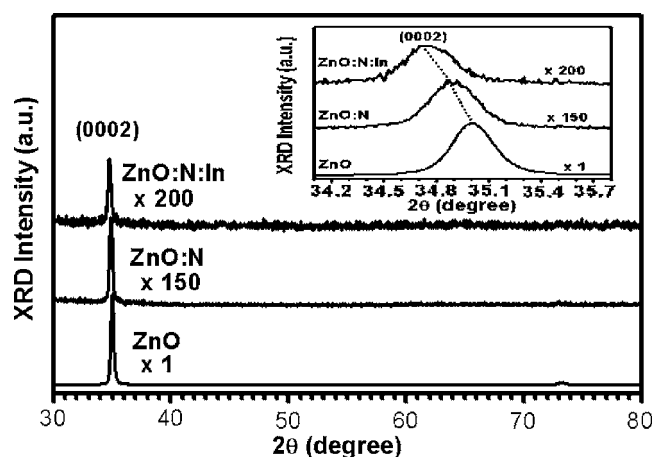


FIG. 1. Normalized XRD patterns of the ZnO, ZnO:N, and ZnO:N:In films with systematic error of $+0.5^\circ$ after a single crystal Si calibration (raw data of 2θ should be reduced by 0.5°).

^{a)} Author to whom correspondence should be addressed; electronic mail: caoyongge@gmail.com

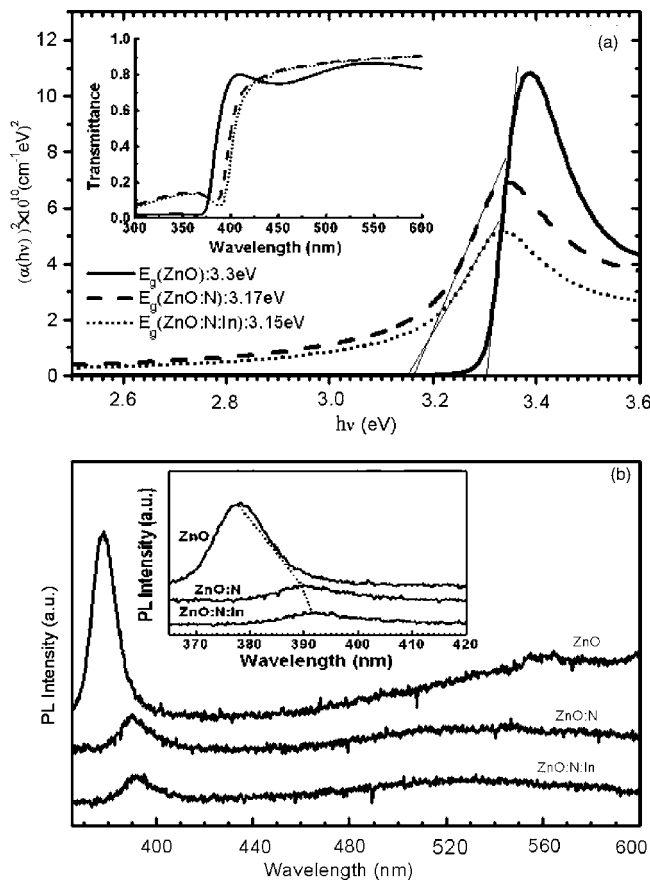


FIG. 2. (a) Transmittance spectra (inset) and the optical direct band gap, and (b) RT PL spectra with magnified NBGE band (inset) of ZnO, ZnO:N, and ZnO:N:In films, respectively.

of the samples. The inset in Fig. 2(a) shows the transmittance spectra of ZnO, ZnO:N, and ZnO:N:In films. All of the three samples are highly transparent in the visible region and have a sharp absorption band in the UV region. The calculated optical band gap [Fig. 2(a)] shows an apparent redshift from 3.30 eV for undoped ZnO film to 3.17 eV for ZnO:N film and finally to 3.15 eV for the ZnO:N:In film, similar to that for the N doped TiO_2 .¹⁹ The Urbach energy width E_0 , which is believed to be a function of structural disorder,²⁰ increases from 73 (ZnO film) to 358 (ZnO:N film) and 360 meV (ZnO:N:In film), demonstrating the decrease in crystallinity of the ZnO films with increasing N incorporation. To double check the band-gap shift and the state of defects in film after N doping, RT photoluminescence (PL) [SPEX 1702/04 Spectrometer, He-Cd laser (325 nm)] has been experimented [see Fig. 2(b)]. The near-band-gap emission (NBGE) in the UV region can be seen, which shows a clear redshift from 3.28 (ZnO film) to 3.18 (ZnO:N film) and 3.16 eV (ZnO:N:In film). The decrease in crystal quality is also substantiated by the decrease in the intensity of the NBGE band after N doping, which may be attributed to the increase in nonradiative recombination from N induced defects. The narrowing of the band gap after N doping may be ascribed to the following effects: (i) the conduction-band renormalization effects due to electron-ionized interaction and electron-ionized impurity interaction,²¹ (ii) merge of the impurity band with the valence or conduction band due to heavy N doping,²² and (iii) the change in ionicity.²³

Table I summarizes the electronic properties of ZnO, ZnO:N, and ZnO:N:In films as characterized by the Hall ef-

TABLE I. Electronic properties of the ZnO, ZnO:N, and ZnO:N:In films fabricated by the sol-gel spin coating method.

Sample	Resistivity ($\Omega \text{ cm}$)	Hall mobility ($\text{cm}^2 \text{ V}^{-1} \text{ s}^{-1}$)	Carrier concentration (cm^{-3})	Type	Substrate
ZnO	3.571	9.8	-1.786×10^{17}	<i>n</i>	Quartz glass
ZnO:N	3.48×10^{-1}	1.3	$+7.506 \times 10^{17}$	<i>p</i>	Quartz glass
ZnO:N:In	1.58×10^{-1}	0.6	$+9.806 \times 10^{17}$	<i>p</i>	Quartz glass

fect measurement (LH 5500PC) at RT. *p*-type conduction for both ZnO:N and ZnO:N:In films is revealed. It is noted that the resistivity of the *p*-ZnO films is very low (of the order of $10^{-1} \Omega \text{ cm}$), which makes them promising for device applications. However, improving hole's mobility of the present *p*-ZnO films is still a challenge. We suspect that the low mobility may result from the decreased crystallinity of the films and the too low annealing temperature (550 °C) for acceptor activation.¹⁰

Having obtained *p*-type ZnO films, we further fabricated *p-n* homojunctions by depositing ZnO and ZnO:N layers (each layer bears a thickness of 400 nm) in tandem onto a quartz glass substrate. Figure 3 shows the *I-V* curves measured at RT for a In/Au/ZnO:N/ZnO/In structure using a semiconductor parameter analyzer (HP4155A). As is shown, the *I-V* result (open circles) is clearly asymmetric with a low turn-on voltage of 1.9 V under the forward bias. The reverse bias breakdown voltage is around 5.8 V. The Ohmic contacts between the ZnO layer and the metal electrodes, i.e., In/ZnO and In/Au/ZnO:N, are confirmed separately by the linear *I-V* relationships (-0.2 – 0.2 mA in the range of -4 – 4 V). Hence the rectifying behavior of the structure originates from the junction at ZnO and ZnO:N interfaces. Fitting the experimental data by the equation $I = I_s [\exp(qV/nkT) - 1]$ for *p-n* junction diodes (the solid line in Fig. 3), we obtain the so called ideality factor $n \sim 24$ [at the low reverse saturation current (I_s) of $2.5 \mu\text{A}$], which is unexpectedly high. Very high ideality factors have also been observed in other non-ideal wide-band-gap *p-n* junctions,²⁴ which may be attributed to the space-charge-limited conduction, deep-level-assisted tunneling, or parasitic rectifying junctions within the device.²⁴ Such *I-V* characteristics are similar to those reported for *p-n* heterojunctions.^{25–27} We would like to also point out that no luminescence is detected from this junction at RT during *I-V* measurements. This is possibly due to (i)

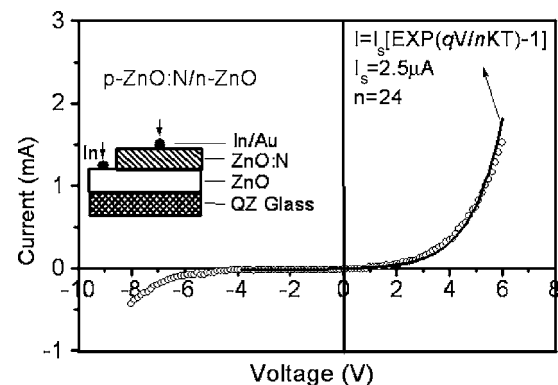


FIG. 3. *I-V* characteristics of a ZnO *p-n* homojunction formed by a 400 nm thick N-doped ZnO layer on a 400 nm thick ZnO layer on a quartz glass substrate. The inset shows the device configuration.

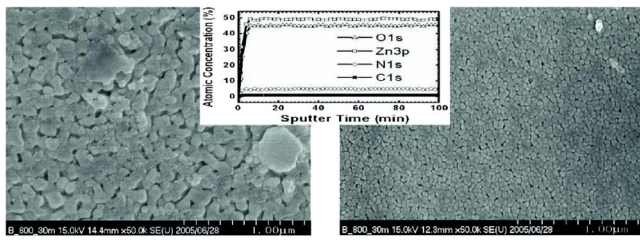


FIG. 4. FESEM morphologies of ZnO (left) and ZnO:N (right) films with the inset of XPS depth profile for the ZnO:N film.

the low mobility of p -ZnO layer,²⁴ (ii) a large portion of the current flows through the grain boundaries in film due to a lower resistivity there rather than within the grains,¹³ or (iii) nonradiative recombination from defects at the interface of the junction.¹³

Return to the data of Table I, one observes a lower resistivity of the p -ZnO films than that of the undoped ZnO film, which seems to be inconsistent with the low mobility and moderate hole density measured. In order to shed some light on the problem and to unveil the cause of unobservable electroluminescence from the p - n junction, samples' surface morphologies and compositions of p -ZnO and n -ZnO films are probed. It is known that an apparent morphological change and a composition variation of semiconductor films can significantly affect their electronic properties. Figure 4 shows the morphology of the undoped ZnO film (left panel) and ZnO:N film (right panel) as measured by a field emission scanning electron microscopy (FESEM; HITACH 95-99 S-4700), while the inset shows x-ray photoelectron spectroscopy (XPS) depth profile for the ZnO:N film. For the latter, nonmonochromatic Mg $K\alpha$ line at 1253.6 eV has been used (ESCA-5700ci, Physical Electronics, Inc.). It can be shown that the grain sizes decrease from 100–300 for the ZnO film to \sim 50 nm for ZnO:N film. The dense films are confirmed by the lack of significant pores and pits in the SEM micrographs. The top-flat grains with hexlike shape suggest the wurtzite structure with (0001) orientation. No typical surface roughening is observable. The XPS depth profile suggests uniform chemical composition in sample. The relative compositions are determined to be 49.3% for Zn, 45.1% of O, 4.8% N, and 0.8% C. Nitrogen incorporation may suppress diffusion of Zn and O atoms to form large grains. As the grain boundary bears lower resistivity than that within the grain for ZnO films,¹³ it is likely that a higher density of grain boundaries in the p -ZnO film will lead to low resistivity film than ZnO (see Table I). Consequently, parasitic series resistances and parasitic rectifying junctions within the p - n homojunction may be introduced, which would then give rise to the high ideality factor (Fig. 3) and poor optical emission. Furthermore, the effects of poorer crystallinity with increasing N doping cannot be ignored. N doping in ZnO layers will induce more defects, which contribute to deep-level-assisted tunneling or act as nonradiative recombination centers. Optimal annealing process may provide an ideal route to solve both of the above problems. High temperature annealing may be essential not only for annihilating nonequilibrium defects but also to activate the acceptors.¹⁰ Unfortunately N doping becomes difficult at high temperatures.

In summary, N-doped and In-N-codoped p -type ZnO films on a quartz glass substrate have been achieved by sol-gel spin coating. The fabricated p -ZnO film exhibits low

resistivity of the order of $10^{-1} \Omega \text{ cm}$, low mobility ($0.6\text{--}1.3 \text{ cm}^2 \text{ V}^{-1} \text{ s}^{-1}$), and moderate hole density [$(7.506\text{--}9.8) \times 10^{17} \text{ cm}^{-3}$]. The increased grain boundaries and decreased crystallinity with increasing N doping level in ZnO may have contributed to its low resistivity and low mobility. The two-layer structured ZnO p - n homojunctions are also prepared and a typical rectifying behavior in I - V curve is observed. However, we do not detect electroluminescence from the junction. An improvement in the mobility of holes in p -ZnO film is still a challenge for future work.

This research was financially supported by the NITECH 21st Century COE Program for World Ceramic Center for Environmental Harmony. The authors greatly acknowledge Professor Dr. M. H. Xie in the University of Hong Kong for improving the quality of this letter.

¹R. F. Service, *Science* **276**, 895 (1997).

²T. Makino, C. H. Chia, T. T. Nguen, and Y. Segawa, *Appl. Phys. Lett.* **77**, 1632 (2000).

³D. C. Look, D. C. Reynolds, C. W. Litton, R. L. Jones, D. B. Eason, and G. Cantwell, *Appl. Phys. Lett.* **81**, 1830 (2002).

⁴A. B. M. A. Ashrafi, I. Suemune, H. Kumano, and S. Tanaka, *Jpn. J. Appl. Phys., Part 2* **41**, L1281 (2002).

⁵K. Minegishi, Y. Koiwai, Y. Kikuchi, K. Yano, M. Kasuga, and A. Shimizu, *Jpn. J. Appl. Phys., Part 2* **36**, L1453 (1997).

⁶Z.-Z. Ye, J.-G. Lu, H.-H. Chen, Y.-Z. Zhang, L. Wang, B.-H. Zhao, and J.-Y. Huang, *J. Cryst. Growth* **253**, 258 (2003).

⁷X.-L. Guo, H. Tabata, and T. Kawai, *J. Cryst. Growth* **237–239**, 544 (2002).

⁸S. J. Jiao, Z. Z. Zhang, Y. M. Lu, D. Z. Shen, B. Yao, J. Y. Zhang, B. H. Li, D. X. Zhao, X. W. Fan, and Z. K. Tang, *Appl. Phys. Lett.* **88**, 031911 (2006).

⁹C.-C. Lin, S.-Y. Chen, S.-Y. Cheng, and H.-Y. Lee, *Appl. Phys. Lett.* **84**, 5040 (2004).

¹⁰A. Tsukazaki, A. Ohtomo, T. Onuma, M. Ohtani, T. Makino, M. Sumiya, K. Ohtani, S. F. Chichibu, S. Fuke, Y. Segawa, H. Ohno, H. Koinuma, and M. Kawasaki, *Nat. Mater.* **4**, 42 (2005).

¹¹M. Joseph, H. Tabata, and T. Kawai, *Jpn. J. Appl. Phys., Part 2* **38**, L1205 (1999).

¹²J. M. Bian, X. M. Li, X. D. Gao, W. D. Yu, and L. D. Chen, *Appl. Phys. Lett.* **84**, 541 (2004).

¹³F. Zhuge, L. P. Zhu, Z. Z. Ye, D. W. Ma, J. G. Lu, J. Y. Huang, F. Z. Wang, Z. G. Ji, and S. B. Zhang, *Appl. Phys. Lett.* **87**, 092103 (2005).

¹⁴Ü. Özgür, Ya. I. Alivov, C. Liu, A. Teke, M. A. Reshchikov, S. Doğan, V. Avrutin, S.-J. Cho, and H. Morkoç, *J. Appl. Phys.* **98**, 041301 (2005).

¹⁵Y. Ma, G. T. Du, S. R. Yang, Z. T. Li, B. J. Zhao, X. T. Yang, T. P. Yang, Y. T. Zhang, and D. L. Liu, *J. Appl. Phys.* **95**, 6268 (2004).

¹⁶J. G. Lu, L. P. Zhu, Z. Z. Ye, F. Zhuge, B. H. Zhao, J. Y. Huang, L. Wang, and J. Yuan, *J. Cryst. Growth* **283**, 413 (2005).

¹⁷S. K. Kim, S. A. Kim, C. H. Lee, H. J. Lee, S. Y. Jeong, and C. R. Cho, *Appl. Phys. Lett.* **85**, 419 (2004).

¹⁸K. Nakahara, H. Takasu, P. Fons, A. Yamada, K. Iwata, K. Matsubara, R. Hunger, and S. Niki, *Appl. Phys. Lett.* **79**, 4139 (2001).

¹⁹R. Asahi, T. Morikawa, T. Ohwaki, K. Aoki, and Y. Taga, *Science* **293**, 269 (2001).

²⁰J. Melsheimer and D. Ziegler, *Thin Solid Films* **129**, 35 (1985).

²¹W. Walukiewicz, *Phys. Rev. B* **41**, 10218 (1990).

²²J. G. Lu, Z. Z. Ye, F. Zhuge, Y. J. Zeng, B. H. Zhao, and L. P. Zhu, *Appl. Phys. Lett.* **85**, 3134 (2004).

²³G. D. Yuan, Z. Z. Ye, L. P. Zhu, Y. J. Zeng, J. Y. Huang, Q. Qian, and J. G. Lu, *Mater. Lett.* **58**, 3741 (2004).

²⁴Y. W. Heo, Y. W. Kwon, Y. Li, S. J. Pearton, and D. P. Norton, *Appl. Phys. Lett.* **84**, 3474 (2004).

²⁵D. K. Hwang, S. H. Kang, J. H. Lim, E. J. Yang, J. Y. Oh, J. H. Yang, and S. J. Parka, *Appl. Phys. Lett.* **86**, 222101 (2005).

²⁶K. Ip, Y. W. Heo, D. P. Norton, S. J. Pearton, J. R. LaRoche, and F. Ren, *Appl. Phys. Lett.* **85**, 1169 (2004).

²⁷Y. I. Alivov, E. V. Kalinina, A. E. Chrenkov, D. C. Look, B. M. Ataev, A. K. Omaev, M. V. Chukichev, and D. M. Bagnall, *Appl. Phys. Lett.* **83**, 4719 (2003).